

INDEPENDENT COMPONENT ANALYSIS (ICA) APPLIED TO LONG BUNCH BEAMS IN THE LOS ALAMOS PROTON STORAGE RING*

J. Kolski[†], R. Macek, R. McCrady, X. Pang, LANL, Los Alamos, NM, 87545, USA

Abstract

Independent component analysis (ICA) is a powerful blind source separation (BSS) method[1]. Compared to the typical BSS method, principal component analysis (PCA), which is the BSS foundation of the well known model independent analysis (MIA)[2], ICA is more robust to noise, coupling, and nonlinearity[3, 4, 5]. ICA of turn-by-turn beam position data has been used to measure the transverse betatron phase and amplitude functions, dispersion function, linear coupling, sextupole strength, and nonlinear beam dynamics[3, 4, 5]. We apply ICA in a new way to slices along the bunch, discuss the source signals identified as betatron motion and longitudinal beam structure, and for betatron motion, compare the results of ICA and PCA.

INTRODUCTION

We apply BSS in a new way to slices along the bunch[6]. We digitize beam signals from the Los Alamos Proton Storage Ring (PSR) for a full injection-extraction cycle, ≥ 1800 turns. We divide the digitized signal into time slices of equal length using the 0.5 ns digitization bin length. The long digitized signal vector is stacked turn-by-turn to form the data matrix

$$\mathbf{x}(t) = \begin{pmatrix} x_1(1) & x_1(2) & \dots & x_1(N) \\ x_2(1) & x_2(2) & \dots & x_2(N) \\ \vdots & \vdots & \ddots & \vdots \\ x_M(1) & x_M(2) & \dots & x_M(N) \end{pmatrix}, \quad (1)$$

such that each row of \mathbf{x} is data from a single time slice for all N turns, and each column of \mathbf{x} is data from all M time slices for a single turn. The slices are located at a fixed longitudinal phase and position along the bunch. The last turn beam profile plotted in Fig. 1 is an example of the last column of \mathbf{x} .

ICA and PCA model \mathbf{x} as a linear combination of independent components (ICs) and principal components (PCs) respectively and yield respectively modes and patterns, describing the source signal's strength in space (along the bunch) and time.

Principal Component Analysis (PCA)

PCA is the simplest of the BSS methods. Many other BSS methods use PCA for preprocessing and noise reduction. PCA was originally applied for beam analysis in the well known MIA.

* Work supported by in part by United States Department of Energy under contract DE-AC52-06NA25396. LA-UR 12-24396

[†] Electronic address: jkolski@lanl.gov

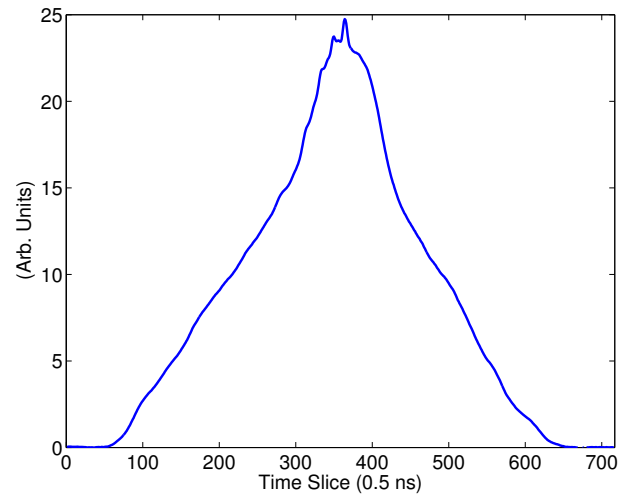


Figure 1: The last turn beam profile as an example of the last column of the data matrix \mathbf{x} in Eq. (1). The PSR's revolution period is 358 ns corresponding to 716 time slices.

PCA identifies patterns in data and expresses the high-dimensional data by highlighting the underlying structures represented as PCs. The PCs are used to compress data by reducing redundant dimensions without much loss of information. PCA minimizes the redundancy measured by covariance, maximizes the signal measured by variance, and results in uncorrelated PCs. Two random variable vectors \vec{y}_1 and \vec{y}_2 are uncorrelated if their covariance is zero,

$$\text{cov}(\vec{y}_1, \vec{y}_2) = \langle \vec{y}_1, \vec{y}_2 \rangle - \langle \vec{y}_1 \rangle \langle \vec{y}_2 \rangle = 0, \quad (2)$$

where $\langle \dots \rangle$ is the expectation value. The core of PCA is singular value decomposition (SVD). SVD of the data matrix \mathbf{x} ($M \times N$) yields eigenvectors \mathbf{U} ($M \times M$) in column-space and \mathbf{V} ($N \times N$) in row-space connected by a diagonal matrix of singular values (SVs) $\mathbf{\Lambda}$ ($M \times N$),

$$\mathbf{x} = \mathbf{U}\mathbf{\Lambda}\mathbf{V}^T. \quad (3)$$

The columns of \mathbf{U} span column-space, the M -dimensional space of time slice number, and are called spatial patterns. The columns of \mathbf{V} span row-space, the N -dimensional space of turn number, and are called temporal patterns. The PCs are ordered by their SVs, which represent their strength.

Independent Component Analysis (ICA)

The objective of ICA is to calculate the L source signals \mathbf{s} ($L \times N$) given the data matrix \mathbf{x} ($M \times N$), but the mixing

matrix \mathbf{A} ($M \times L$) is unknown

$$\mathbf{x} = \mathbf{A}\mathbf{s}. \quad (4)$$

ICA assumes independent source signals, a stricter requirement than PCA. Two random variable vectors \vec{y}_1 and \vec{y}_2 are independent if the covariance of any function of \vec{y}_1 and any function of \vec{y}_2 is zero,

$$\langle f(\vec{y}_1), g(\vec{y}_2) \rangle - \langle f(\vec{y}_1) \rangle \langle g(\vec{y}_2) \rangle = 0. \quad (5)$$

For time series data, source signal independence is related to diagonality of covariance matrices[7]. The auto-covariance of a signal is $cov(\vec{y}_i(t), \vec{y}_i(t - \tau))$, where τ is a time lag, $\tau = 0, 1, 2, \dots$. Similarly, the covariance between two signals is $cov(\vec{y}_i(t), \vec{y}_j(t - \tau))$ where $i \neq j$. Applying these two results to mean-zero signals for reasons to become evident later, we write the time-lagged covariance matrix

$$\mathbf{C}_y(\tau) = \langle \mathbf{y}(t)\mathbf{y}(t - \tau)^T \rangle. \quad (6)$$

Source signal independence requires the time-lagged covariance matrices $\mathbf{C}_s(\tau) = \langle \mathbf{s}(t)\mathbf{s}(t - \tau)^T \rangle$ be diagonal,

$$\langle \mathbf{s}_i(t)\mathbf{s}_j(t - \tau)^T \rangle = 0, \quad i \neq j, \quad \tau = 0, 1, 2, \dots \quad (7)$$

It follows that $\mathbf{A}^{-1}\mathbf{x}$ must also possess diagonal time-lagged covariance matrices. The BSS problem is solved by obtaining a demixing matrix that diagonalizes the time-lagged covariance matrices of \mathbf{x} .

The zero time-lagged covariance matrix $\mathbf{C}_x(\tau = 0)$ does not contain enough information to obtain the mixing matrix \mathbf{A} . The key is to utilize the additional information contained in the time-lagged covariance matrices $\mathbf{C}_x(\tau)$. Including more than one time lag improves ICA's performance by resolving degenerate SVs, but it introduces an additional complication of simultaneously diagonalizing many $\mathbf{C}_x(\tau)$. A numerical technique for simultaneously diagonalizing several matrices with Jacobi angles is discussed in Ref. [8]. Typically, 20 - 50 time lags are required to separate source signals with close SVs[4, 5]. We use the ICA algorithm Second Order Blind Identification (SOBI)[7], which accommodates multiple time lags, in our analysis and outline the algorithm below:

1. Whitening

The data matrix \mathbf{x} is preprocessed to obtain mean-zero, whitened ($\mathbf{y}\mathbf{y}^T = \mathbf{I}$) data. Mean-zero data, which simplifies the covariance matrix calculation, is calculated by subtracting the average over the temporal variation. SVD is applied to the zero time-lagged covariance matrix of the mean-zero data matrix $\bar{\mathbf{x}}$

$$\begin{aligned} \mathbf{C}_{\bar{\mathbf{x}}}(0) &= \langle \bar{\mathbf{x}}(t)\bar{\mathbf{x}}(t)^T \rangle \\ &= (\mathbf{U}_1, \mathbf{U}_2) \begin{pmatrix} \Lambda_1 & 0 \\ 0 & \Lambda_2 \end{pmatrix} \begin{pmatrix} \mathbf{U}_1^T \\ \mathbf{U}_2^T \end{pmatrix}, \end{aligned} \quad (8)$$

where Λ_1 and Λ_2 are diagonal matrices of SVs separated by a cutoff threshold λ_c such that $\min(\text{diag}[\Lambda_1]) \geq \lambda_c \geq$

$\max(\text{diag}[\Lambda_2])$. The cutoff threshold λ_c is determined by the number of SVs L included in the analysis. \mathbf{U}_1 and \mathbf{U}_2 are eigenvectors corresponding to Λ_1 and Λ_2 respectively. The mean-zero, whitened data is calculated

$$\mathbf{z} = \mathbf{Y}\bar{\mathbf{x}}, \quad (9)$$

where $\mathbf{z}\mathbf{z}^T = \mathbf{I}$, $\mathbf{Y} = \Lambda_1^{-1/2}\mathbf{U}_1^T$, and $\Lambda_1^{-1/2}$ indicates the inverse square root of the diagonal elements individually.

2. Joint diagonalization

The time-lagged covariance matrices of the mean-zero, whitened data matrix \mathbf{z} are calculated for a set of time lags ($\tau_k, k = 0, 1, \dots, K$)

$$\mathbf{C}_z(\tau_k) = \langle \mathbf{z}(t)\mathbf{z}(t - \tau_k)^T \rangle. \quad (10)$$

Modified time-lagged covariance matrices $\bar{\mathbf{C}}_z(\tau_k)$ are constructed from $\mathbf{C}_z(\tau_k)$

$$\bar{\mathbf{C}}_z(\tau_k) = (\mathbf{C}_z(\tau_k) + \mathbf{C}_z(\tau_k)^T) / 2. \quad (11)$$

SVD is well defined, since $\bar{\mathbf{C}}_z(\tau_k)$ is real and symmetric

$$\bar{\mathbf{C}}_z(\tau_k) = \mathbf{W}\mathbf{D}_k\mathbf{W}^T, \quad (12)$$

where \mathbf{W} is the unitary demixing matrix and \mathbf{D}_k is a diagonal matrix. The Jacobi angle technique discussed in Ref. [8] is used to find the demixing matrix \mathbf{W} , which is a joint diagonalizer for all $\mathbf{C}_z(\tau_k)$. The mixing matrix \mathbf{A} and the source signals \mathbf{s} are calculated

$$\mathbf{A} = \mathbf{Y}^{-1}\mathbf{W} \quad \text{and} \quad \mathbf{s} = \mathbf{W}^T\mathbf{Y}\bar{\mathbf{x}}. \quad (13)$$

The columns of \mathbf{A} span column-space, the M -dimensional space of time slice number, and are called spatial modes. The rows of \mathbf{s} span row-space, the N -dimensional space of turn number, and are called temporal modes.

INDEPENDENT COMPONENTS

We digitize beam signals from a short stripline beam position monitor (BPM) with 400 MHz peak frequency response. We digitize the BPM's vertical sum and difference signals for BSS.

We typically ran our SOBI analysis for $L = 30$ SVs, $K = 50$ time lags, and as many turns as possible.

ICs are presented in several graphs; see Fig. 2:

- Top left** spatial mode (blue), last turn beam profile (green).
- Bottom left** fft of spatial mode (top left), peak integer revolution harmonic, resolution (1/1).
- Top center** integrated spatial mode (top left) (blue), last turn beam profile (green).
- Bottom center** correlation of IC and $\mathbf{z}(t - \tau)$, SV.
- Top right** temporal mode ($-1 =$ last turn), fractional revolution harmonic from sinusoid fit.
- Bottom right** fft of temporal mode (top right), peak fractional revolution harmonic, resolution (1/N).

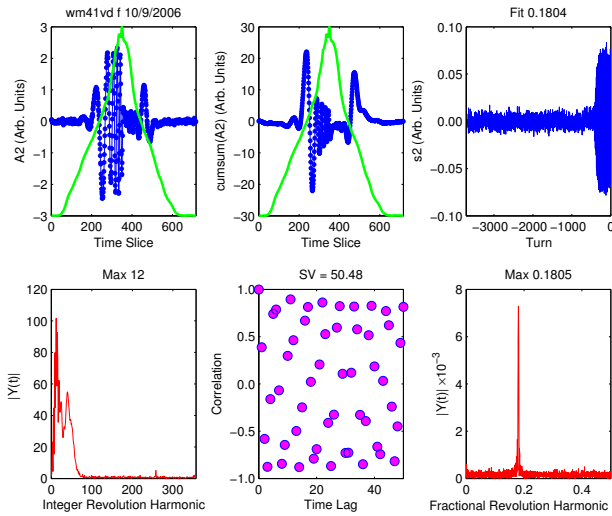


Figure 2: Typical betatron IC resulting from ICA of the difference signal for a single-turn kick.

Betatron ICs

In previous applications, ICA obtains quality ICs representing betatron motion [3, 4, 5], so the betatron IC result from slices along the bunch is of interest. We induce coherent betatron oscillation with a single-turn kick. The beam is stored for 420 turns ($150 \mu\text{s}$) after the kick.

The IC in Fig. 2 is identified as betatron motion because the fractional revolution harmonic (bottom right) is close to the operating fractional betatron tune value 0.1805 and because the temporal mode (top right) is only nonzero for turns after the single-turn kick.

The spatial mode (top left) indicates the strength of the 0.1805 fractional betatron tune oscillation along the beam bunch. However, in this case it is easier to interpret the integrated spatial mode (top center) because it has units proportional to current, whereas the spatial mode has units proportional to the derivative of the current. The integrated spatial mode maximums indicate that the majority of particles undergoing coherent betatron motion with a fractional tune of 0.1805 are located symmetric about the bunch center at time slices 237 and 474 and represent the coherent space charge tune shifted beam. The fast oscillation slightly forward of the bunch center describes mixing of betatron tunes for the central time slices.

We wish to compare the 15 identified betatron ICs with each other and with the $\text{FFT}(\mathbf{x})$. We define the greatest strength location to be the fractional revolution harmonic and time slice where an IC is strongest. The time slice coordinate is determined by the integrated spatial mode (top center) maximum. We calculate a leading and trailing edge greatest strength location for each IC and compare with $\text{FFT}(\mathbf{x})$ in Fig. 3. The greatest strength locations of the 15 betatron ICs reproduce the tune distribution along the bunch. The spatial mode (top left) in Fig. 2 replicates the 0.1805 fractional tune contour along the bunch of the tune

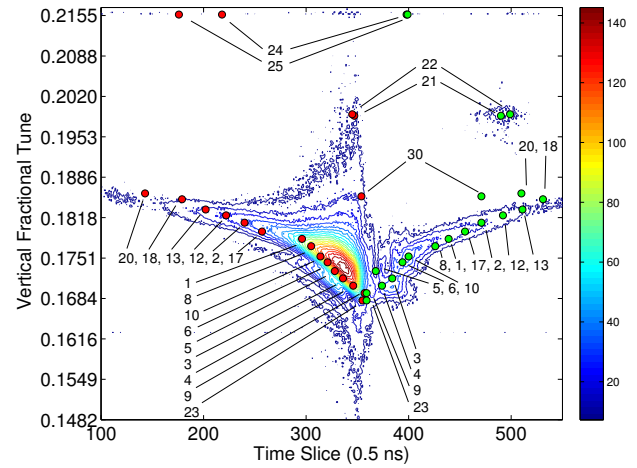


Figure 3: Betatron tune along the bunch and the greatest strength location for the first 30 ICs, some of which lie outside the plot boundary. The contour plots $\text{FFT}(\mathbf{x})$ along turn for each time slice. The red and green circles mark the leading and trailing edge greatest strength locations respectively with IC number indicated by numeric labels. The beam profile peak is located at time slice 350.

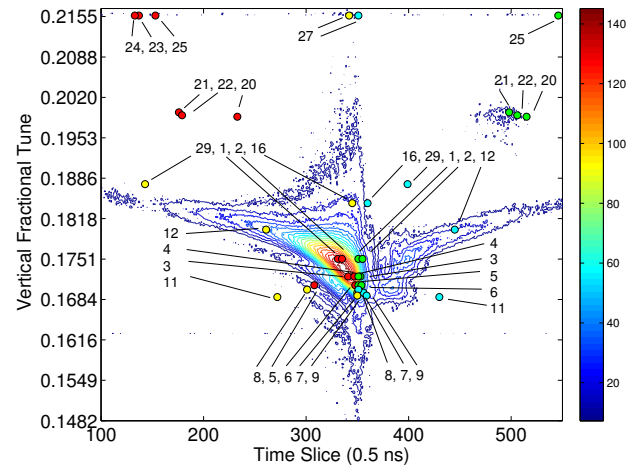


Figure 4: Betatron tune along the bunch and the greatest strength location for the first 30 PCs, some of which lie outside the plot boundary. The contour plots $\text{FFT}(\mathbf{x})$ along turn for each time slice. The red (yellow) and green (cyan) circles mark the leading and trailing edge greatest strength locations respectively for PCs with dominant betatron motion (dominant source signal other than betatron motion). A numeric label indicates PC number. The beam profile peak is located at time slice 350.

distribution in Fig. 3. The betatron ICs must be viewed in concert as in Fig. 3 to obtain the full picture of the coherent space charge tune shift along the bunch.

We compare the PCA result with $\text{FFT}(\mathbf{x})$ in Fig. 4. We include in Fig. 4 all PCs with mixed betatron motion. Most

betatron PCs have peak strengths located near the bunch center where the difference signal is largest because PCA is unable to diagonalize the frequency continuum beyond its peak strength and average location. It is clear from Fig. 4 that PCA is unable to recover the coherent space charge tune shift along the bunch.

201.25 MHz IC

The 201.25 MHz IC represents the longitudinal structure of beam newly injected in the PSR, Fig. 5. The 201.25 MHz IC is identified by the character of its temporal mode (top right), which has constant amplitude for the first 1400 turns and suddenly reduces to noise for the last 500 turns. The reduction coincides with the end of accumulation.

The total revolution harmonic is 72.07136 as expected because the PSR design revolution frequency is the 72.07 subharmonic of the 201.25 MHz linac frequency. Multiplying the total revolution harmonic by the revolution frequency yields exactly 201.25 MHz. The 0.07 fractional revolution harmonic describes the 14 turn rastering period of the longitudinal phase space painting executed during injection.

The power of ICA, which lies in the spatial mode (top left), is most prominent in this example. The spatial mode describes the longitudinal phase of the injected beam. The spatial mode is constant amplitude across the injection region and zero outside. The spatial mode also describes the injection length each turn (pattern width). The spatial mode is a sinusoidal oscillation with period 5 ns, a 201.25 MHz period, and 58 peaks. Each peak represents a single linac pulse (linac RF bucket) injected into the PSR. The injection pattern width is 290 ns, which divided by the 201.25 MHz period yields 58 linac pulses injected per turn as indicated by the spatial mode peaks.

We now examine additional examples of the spatial

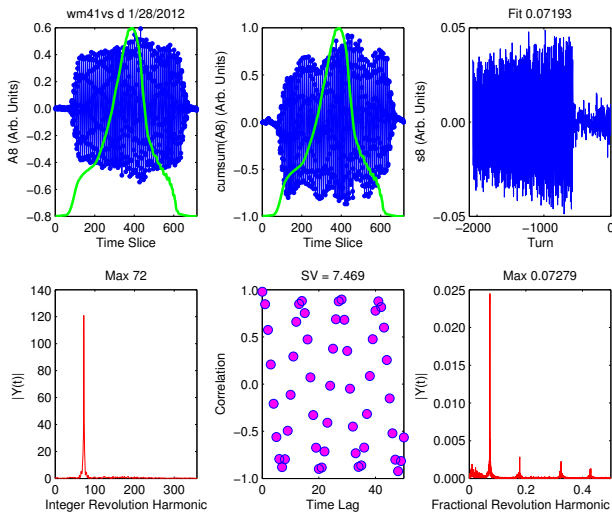


Figure 5: Typical 201.25 MHz IC resulting from ICA of the sum signal.

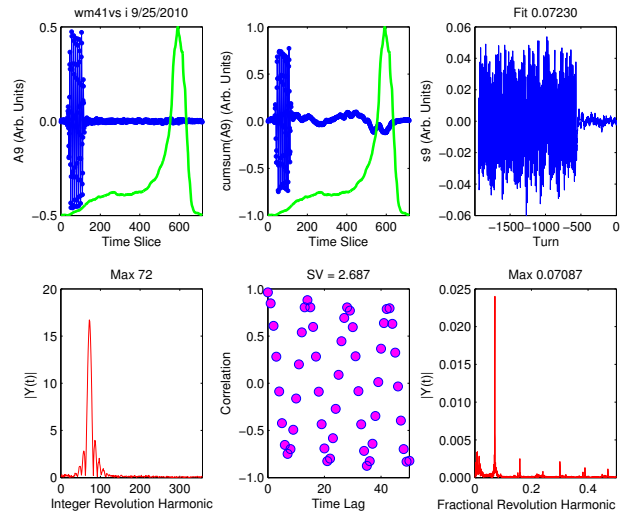


Figure 6: The 201.25 MHz IC resulting from ICA of the sum signal when injecting a 50 ns pattern width beam 120° early in the PSR’s RF bucket.

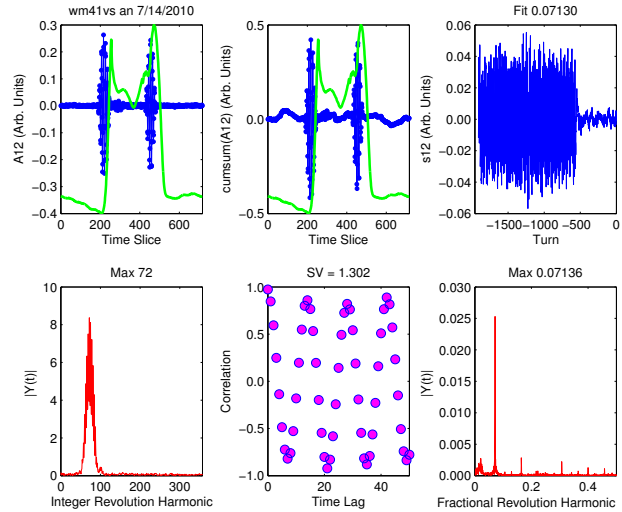


Figure 7: The 201.25 MHz IC resulting from ICA of the sum signal when injecting beam with a notch.

mode (top left) produced from beam signals collected under different injection schemes. The IC plotted in Fig. 6 was produced from beam signal collected while injecting a 50 ns pattern width beam 120° early in the PSR’s RF bucket. The injection region of the spatial mode is 100 time slices wide, corroborating the pattern width. Additionally, the spatial mode’s position has shifted forward, confirming early injection. The last turn profile indicates that after 200 μs of storage the majority of beam is located opposite in the RF bucket of where it was injected.

The IC plotted in Fig. 7 was produced from beam signals collected while injecting with a “notch” in the beam, illustrated by the spatial mode (top left). The injection region

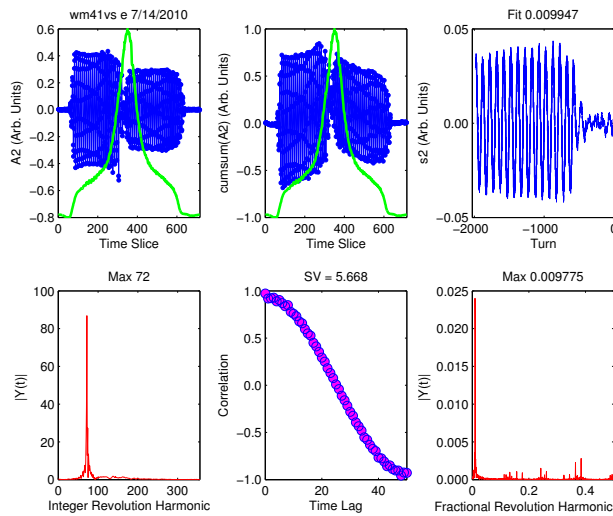


Figure 8: 201.25 MHz IC resulting from ICA of the sum signal when the revolution frequency is near an integer sub-harmonic of the linac frequency.

widths are 60 time slices, and the notch width between the two injection regions is 180 time slices. The spatial mode reproduces the notch injection scheme: inject for 30 ns, no injection for 90 ns (notch), and inject for 30 ns.

At the beginning of the 2010 LANSCE production run cycle, we observed an unusual amount of “hash” noise-like structure on the PSR beam profile. The hashy beam profile is an operational concern because it could excite longitudinal microwave instabilities and other longitudinal space charge effects[9, 10]. We wished to remove the hash from the beam profile, but did not know where to look for the cause, so we took data for ICA. ICA of the hashy beam signal yields the 201.25 MHz IC plotted in Fig. 8, which is reminiscent of Fig. 5 with obvious difference in the temporal mode (top right). A fractional revolution harmonic 0.009 describes an oscillation that repeats every 111 turns. The slow injection rastering causes the hashy beam profile by longitudinally stacking the beam upon itself more than in nominal operations where the fractional revolution harmonic is 0.07.

We calculate the PSR revolution frequency from the IC plotted in Fig. 8. The unchanging 201.25 MHz linac frequency is divided by the total revolution harmonic 72.009. This results in a revolution frequency of 2.7948 MHz. However, the PSR design revolution frequency is 2.7924 MHz. The revolution frequency differs from design by 2.4 kHz causing the hash on the current profile.

The PSR revolution frequency is created by a frequency generator into which a value is typed. For this run, the frequency generator value was inadvertently set to 2.7948 MHz; exactly the number predicted by ICA.

CONCLUSIONS

We adopt a new method applying ICA to slices along the beam and test with PSR sum and difference beam position signals digitized for an entire injection-extraction cycle.

We determine that PCA is inadequate for the BSS problem of slices along the bunch because PCA is unable to completely separate the source signals, yielding PCs describing a mixture of two or more source signals.

We discuss two classes of ICs identified by spatial and temporal modes. When viewed in concert, the ICs describing betatron motion along the pulse yielded the coherent space charge tune shift. Another IC described the longitudinal structure of newly injected beam and gave the longitudinal phase of injection and the revolution frequency.

REFERENCES

- [1] A. Hyvärinen, et al., (John Wiley & Sons, New York, 2001).
- [2] J. Irwin, et al., Phys. Rev. Lett. **82**, 1684 (1999); C.X. Wang, Ph.D. thesis, unpublished (Stanford University 1999).
- [3] X. Huang, et al., PR-STAB **8**, 064001 (2005); X. Huang, Ph.D. thesis, unpublished (Indiana University 2005).
- [4] F. Wang and S.Y. Lee, PR-STAB **11**, 050701, (2008); F. Wang, Ph.D. thesis, unpublished (Indiana University 2008).
- [5] X. Pang and S.Y. Lee, Journal of Applied Physics, **106**, 074902 (2009); X. Pang, Ph.D. thesis, unpublished (Indiana University 2009).
- [6] J. Kolski, et al., IPAC 2012 Conference Proceedings, WEPPR038, May 2012; J. Kolski, Ph.D. thesis, unpublished (Indiana University 2010).
- [7] A. Belouchrani, et al., IEEE Trans. Signal Processing, **45**, 434-444, (1997).
- [8] J.F. Cardoso and A. Souloumiac, SIAM J. Mat. Anal. Appl., **17**, 161, (1996).
- [9] C. Beltran, et al., PAC 2003 Conference Proceedings, TOPD004, May 2003; C. Beltran, Ph.D. thesis, unpublished (Indiana University 2003).
- [10] R. McCrady, et al., LANSCE-ABS 06-008, PSR 06-002 (unpublished).